Biosystems Engineering (2006) **95** (4), 507–515
doi:10.1016/j.biosystemseng.2006.08.006
PM—Power and Machinery

Dynamic Friction Coefficient Measurement of Granular Fertiliser Particles

T.E. Grift[1]; G. Kweon[1]; J.W. Hofstee[2]; E. Piron[3]; S. Villette[4]

[1]Department of Agricultural and Biological Engineering, University of Illinois, Urbana IL, USA; e-mail of corresponding author: grift@uiuc.edu
[2]Wageningen University and Research Centre, Wageningen, The Netherlands; e-mail: JanWillem.Hofstee@wur.nl
[3]Agricultural and Environmental Engineering Research Institute (CEMAGREF), Montoldre, France;
e-mail: emmanuel.piron@clermont.cemagref.fr
[4]Etablissement National d'Enseignement Supérieur Agronomique (ENESAD), Dijon, France; e-mail: s.villette@enesad.fr

(Received 26 December 2005; accepted in revised form 17 August 2006; published online 13 October 2006)

Theoretically, in the absence of friction, when a particle is sliding along a straight radial vane, mounted on a flat disc which is spinning at a constant rotational velocity, its radial and tangential velocity are equal at any point along the vane. In reality, there are disturbances causing a difference between the radial and tangential velocities, such as drop mechanics, mechanical (Coulomb) friction, aerodynamic effects, as well as particle bouncing effects against the vane and other particles. These factors were lumped together and termed the 'friction coefficient'.

The tangential particle velocity at the discharge point was assumed constant, since the particle was assumed in direct contact with the vane until emanation. The radial particle velocity was measured at a distance of 0·4 m from the disc edge with an optical sensor developed in earlier research. A theoretical analysis was used to obtain equations that allowed determination of the mechanical friction coefficient of individual particles, based on the measured radial velocity and the assumed constant tangential velocity.

For experiments, a commercial single disc spreader fitted with a flat disc and straight radial vanes was used. The results for urea fertiliser showed a near-Gaussian distribution of the friction coefficients, with a mean value of 0·36 and a standard deviation of 0·1 among 812 measurements. In addition, an inversely proportional relationship was found between the friction coefficients and the particle diameters.

1. Introduction

The application of granular fertiliser has traditionally been carried out with equipment that mimics a human arm swing such as the spinner disc design. Spinner-type spreaders have major advantages; they are simple in design, easy to use and maintain, reliable, inexpensive and they have a high field capacity. However, the quality of the resulting spread pattern in the field can be poor, owing to improper overlapping, variations in physical properties of the fertiliser, hill slopes, unfavourable weather conditions such as high winds, ill adjusted spreaders and poorly designed spreaders such as the single spinner-type. These factors can lead to under application, causing reduced crop yield and over application, which is uneconomic, can lead to crop damage, and have environmental impacts, such as leaching of chemicals into the ground water (Helms *et al*., 1987). Most of these problems can be avoided by having properly maintained and calibrated equipment. However, there is an inherent problem with spinner type fertiliser spreaders: the pattern uniformity depends highly on the application rate (Parish, 2002). Fulton *et al*. (2001) performed a large-scale investigation on the rate and uniformity of a spinner-type spreader using the ASAE standardised collection tray method (ASAE, 1999). A dual disc spinner type spreader was started at a low application rate of 56 kg ha^{-1}, which was gradually increased to the maximum rate of 168 kg ha^{-1}. The resulting spread pattern changed from a desirable Gaussian shape at the low application rate to an M-shape at the medium setting to a W-shape at the highest application rates. M- and W-shapes have a devastating effect on the pattern uniformity and robustness (Grift,

Notation

A,B,	integration constants
D	distance from the sensor to the disc edge, m
F_g	Gravity force acting on fertiliser particle, N
F_{cor}	Coriolis force acting on fertiliser particle, N
g	gravitation acceleration, m s^{-2}
L_{AIR}	travel distance from discharge location to sensor, m
m	mass of fertiliser particle, kg
R	radius of the disc, m
t	time, s
u_{TAN}	tangential discharge velocity at distance D from disc edge, m s^{-1}
u_{RAD}	measured radial discharge velocity at distance D from disc edge, m s^{-1}
u_{TOT}	total discharge velocity at distance D from disc edge, m s^{-1}
v_{TAN}	tangential discharge velocity at disc edge, m s^{-1}
v_{RAD}	measured radial discharge velocity at disc edge, m s^{-1}
v_{TOT}	total discharge velocity at disc edge, m s^{-1}
x	distance of particle along vane, m
$\dot{x}$	time derivative (velocity) of particle distance along the vane, m s^{-1}
$\ddot{x}$	second time derivative (acceleration) of particle distance along the vane, m s^{-2}
α	discharge angle, rad
β	sensor angle, rad
ε	friction angle, rad
κ	exponential coefficient, function of friction coefficient by definition
μ	friction coefficient of fertiliser particle along vane
ω	rotational velocity of the disc, rad s^{-1}

2000; Grift *et al.*, 2000). The research by Fulton and Parish shows that the spinner design is unsuitable for variable rate application of fertiliser, unless the spreader is fitted with a proper feedback control system such as proposed by Grift and Hofstee (2002).

There are many parameters, influencing the performance of a spinning disc fertiliser spreader such as geometries (disc size and shape, material drop location, shape and size of the feed gates, shape, length and orientation of the vanes), rotational disc velocity, material properties, and environmental conditions such as wind speed and direction, temperature and moisture levels. The spread pattern uniformity is relatively insensitive to some variations such as the rotational velocity of the disc, which merely scales the spread pattern radially. In contrast, variability in the mechanical (Coulomb) friction of the particles against the vanes has a distinct effect on the spread pattern. An increased friction coefficient causes the particles to remain longer on the disc and be discharged at a larger angle with respect to the drop location. This means that apart from a shorter throw distance, the pattern rotates along a vertical axis, which causes major changes in the uniformity. If the friction coefficient of particles could be measured in real time as is proposed in this research, this would allow adjusting the spreader and control the spread pattern under changing material properties.

Many researchers have attempted to measure the mechanical friction coefficient of fertiliser particles in a laboratory setting. Hofstee (1992) measured the dynamic friction coefficient by bringing individual particles in contact with a rotating disc, while measuring normal and friction forces. Aphale *et al.* (2003) used a static inclined plate approach proposed by Cunningham (1963) where several particles were attached to a wooden background and the plate was inclined until the particles began to slide. Modelling approaches such as reported in Dintwa *et al.* (2004a), omitted the absolute value of the friction coefficient altogether, and for the model validation Dintwa *et al.* (2004b) obtained the friction coefficient from personal communications. Olieslagers *et al.* (1996) adopted a value of 0·3, close to the average values as determined by Hofstee (1992). Villette (2005) used a machine vision system to determine the friction angle between the radial and tangential velocity components of particles. Friction coefficient values were obtained for ammonium nitrate, nitrogen phosphorous potassium, and potassium chloride as 0·17, 0·2 and 0·4, respectively.

Aphale *et al.* (2003) note 'although the on-spinner motion is relatively sensitive to the friction coefficient for pure-sliding conditions, using a specific value for the friction coefficient seems unwarranted since accurate determination of this parameter is difficult, especially for materials and spinner plates used in practice'. The research as reported here addresses this very issue.

A method is proposed where the radial velocity of particles is measured at a distance of 0·4 m from the disc edge and the friction coefficient is computed for individual particles passing a velocity/diameter sensor. Theoretically, for a flat disc with straight radial vanes whilst ignoring aerodynamic and mechanical friction, the radial and tangential velocities of particles sliding along the vane are equal at any location along the vane.

Since the particles are assumed to be in contact with the vane until being emanated, their tangential particle discharge velocities can simply be obtained by knowing the constant tangential velocity of the vane at the disc edge. Since the radial velocity of the particles was measured, the friction coefficient was inferred by comparing the measured radial and tangential velocity of the particles. Since the sensor also measures the particle diameters, these were correlated with the friction coefficients as well. The effect of aerodynamics-induced forces on particles during acceleration is a poorly understood process, and therefore, in this study they were ignored and effectively assumed an integral part of the lumped friction coefficient parameter.

Although the research here was limited to particles sliding along a straight radial vane mounted on a flat disc, the method also applies to pitched vanes as well as conical discs by using the appropriate dynamic model and associated friction coefficient measurement equations. Villette *et al.* (2005) showed the mathematical framework to translate the findings of this research to alternative disc and vane configurations.

The objectives of this research were: (1) to determine the friction coefficient of individual urea fertiliser particles in real time; and (2) to investigate the relationship of the friction coefficients with particle diameters.

2. Materials and methods

2.1. *Theoretical analysis*

In this section the equations needed to determine the friction coefficient of fertiliser particles are presented. For a detailed derivation, see Appendix A.

Figure 1 shows the disc/vane geometry and velocity vectors of particles being discharged after acceleration along a straight radial vane. The tangential discharge velocity v_{TAN} in $\mathrm{m\,s^{-1}}$ at the discharge point is a constant equal to the local tangential velocity of the vane since the particle was assumed in contact with the vane until being discharged leading to

$$v_{TAN} = \omega R \tag{1}$$

where ω in $\mathrm{rad\,s^{-1}}$ is the rotational velocity of the disc/vane and R in m is the radius of the disc. The radial discharge velocity v_{RAD} in $\mathrm{m\,s^{-1}}$ is equal to

$$v_{RAD} = \kappa\omega R \tag{2}$$

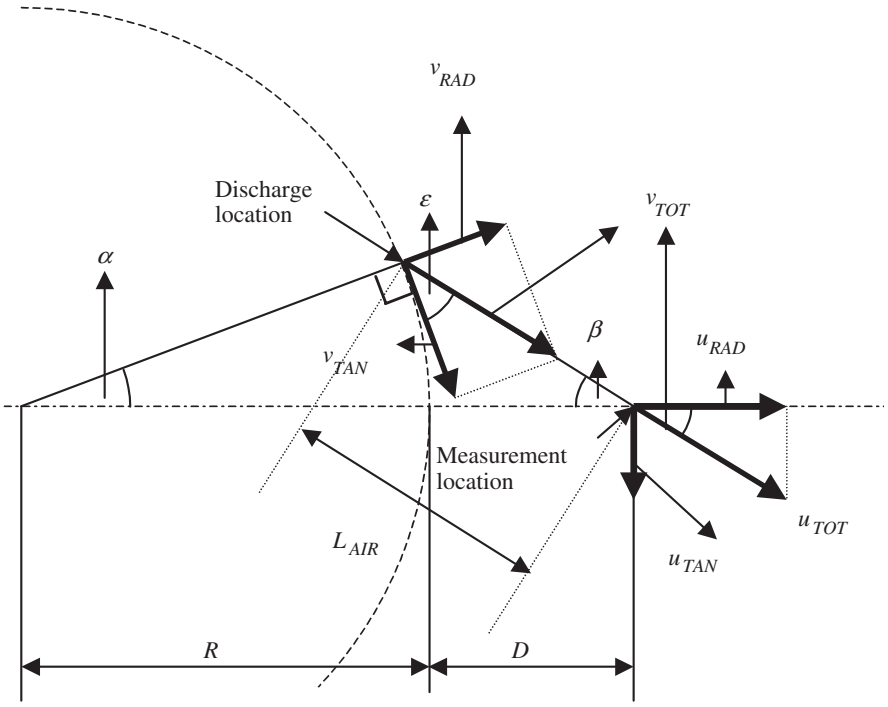

Fig. 1. Schematic of particle velocities at the discharge location (disc edge) as well as the measurement location. The disc is assumed to spin clockwise at a constant rotational velocity of ω $\mathrm{rad\,s^{-1}}$. v_{RAD}, *radial velocity at the discharge location;* v_{TAN}, *tangential velocity at the discharge location;* u_{RAD}, *radial velocity at the measurement location;* u_{TAN}, *tangential discharge velocity;* ε, *friction angle;* β, *sensor angle;* α, *discharge angle;* R, *radius of the disc;* D, *radial distance between the disc edge and the sensor location and* L_{AIR}, *distance of travel through air from the discharge location to the measurement location, since no aerodynamic friction is taken into account, the total velocity at the discharge point* v_{TOT} *is equal to the total velocity at the measurement point* u_{TOT}

where κ is a constant termed the exponential coefficient which is related to the friction coefficient as follows

$$\kappa = -\mu + \sqrt{\mu^2 + 1} \tag{3}$$

In Eqn (3), μ is the Coulomb friction coefficient between the particle and the vane. The total discharge velocity v_{TOT} in m s^{-1} follows from the vector sum of the radial and tangential components given in Eqns (1) and (2)

$$v_{TOT} = \omega R\sqrt{1 + \kappa^2} \tag{4}$$

Aerodynamic friction during acceleration as well as travel through air was ignored implying that the total measured velocity at the sensor is equal to the total discharge velocity

$$u_{TOT} = v_{TOT} = \omega R\sqrt{1 + \kappa^2} \tag{5}$$

Splitting the total measured velocity at the sensor into perpendicular components leads to a measured tangential velocity u_{TAN} in m s^{-1} as follows

$$u_{TAN} = \omega R\frac{R}{R + D} \tag{6}$$

where D in m is the radial distance between the sensor location and the disc edge. Equation (6) implies that the tangential velocity at the sensor u_{TAN} according to theory is constant. The measured radial velocity at the sensor u_{RAD} in m s^{-1} was derived as

$$u_{RAD} = \omega R\left[1 + \kappa^2 - \left(\frac{R}{R + D}\right)^2\right]^{1/2} \tag{7}$$

Solving this equation for the exponential coefficient κ yields:

$$\kappa = \left[\left(\frac{u_{RAD}}{\omega R}\right)^2 + \left(\frac{R}{R + D}\right)^2 - 1\right]^{1/2} \tag{8}$$

Equation (8) shows that the exponential coefficient is solely related to the measured radial velocity u_{RAD} and the constants ω,R,D. Solving Eqn (3) for the friction coefficient μ and substituting the exponential coefficient κ from Eqn (8) yields the friction coefficient as

$$\mu = \frac{1}{2}\left(\frac{1}{\kappa} - \kappa\right) \tag{9}$$

The friction angle ε in rad was defined as the inverse tangent of the exponential coefficient as follows

$$\varepsilon = \tan^{-1}\left(\frac{v_{RAD}}{v_{TAN}}\right) = \tan^{-1}(\kappa) \tag{10}$$

The sensor angle β in rad was found through simple geometry as

$$\beta = \sin^{-1}\left[\frac{R}{(R + D)}\frac{1}{\sqrt{1 + \kappa^2}}\right] \tag{11}$$

The discharge angle α in rad followed from the sum of angles in a triangle

$$\alpha = \frac{\pi}{2} - \varepsilon - \beta \tag{12}$$

The total distance through which the particles travel in air L_{AIR} in m is related to the exponential coefficient and consequently the friction coefficient as well as the constants ω,R,D as follows

$$L_{AIR} = \frac{1}{\sqrt{1 + \kappa^2}}\left[(R + D)\sqrt{1 + \kappa^2 - \left(\frac{R}{R + D}\right)^2} - \kappa R\right] \tag{13}$$

In summary, assuming that the values of the constants ω,R,D are known, the equations show that measuring the radial discharge velocity u_{RAD} in m s^{-1} at a radial distance D in m from the disc edge is sufficient to compute the friction coefficient μ as well as the friction angle ε, the sensor angle β, the discharge angle α and the total travel length in air between the discharge location and the sensor location L_{AIR} in m.

2.2. *Experimental arrangement*

To evaluate the method of friction coefficient measurement, experiments were carried out with a modified Lowery 300 single spinner fertiliser spreader. To accommodate a flat disc, straight radial vane model, the spreader was fitted with a flat galvanised steel disc, and four straight radial vanes. *Figure 2* shows a photo of the arrangement, where in the background, the optical sensor, which measures the radial particle velocities, is visible (Grift & Hofstee, 1997). This sensor was used in

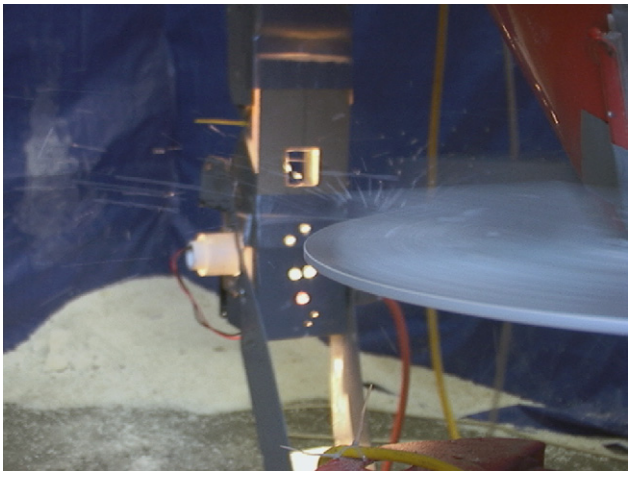

Fig. 2. Spinning flat disc arrangement with straight vanes and optical sensor in background

earlier research to predict the spread pattern of a fertiliser spreader (Grift & Hofstee, 2002).

In the experiments, the existing feed gates were removed and particles were dropped from a narrow (1 cm) vertical slit onto the disc. The disc was spinning at 78 rad s^{-1}, the radius of the disc was 0·245 m, and the radial distance between the disc edge and the sensor D was 0·4 m. During the test, the sensor was rotated around the spreader to scan the complete spreading zone. The friction coefficients were determined using Eqns (8) and (9) which directly linked the measured radial velocity to the friction coefficient of the particles.

3. Results and discussion

Figure 3 shows the measured radial discharge velocity and friction coefficient *versus* the particle diameters out of 812 measurements. Originally, the dataset contained 1096 particles, but many had distinctly lower velocities that were assumed to not have accelerated smoothly along the vane, but being launched upward on impact. The data show a slight diameter dependency of the velocity as well as the friction coefficient, which drops from approximately 0·375 for the smallest measured diameter (1·3 mm) to 0·316 for the largest diameter (3·85 mm). The results also show a highly variable radial discharge velocity. This is in stark contrast to the tangential discharge velocity, which is assumed constant. Since it seems logical that at least some of the effects that contribute to the radial velocity variability also act in the tangential direction, measuring the tangential velocity separately in the future may identify the origin of variability in either direction.

Figure 4 shows histograms of both the measured radial particle velocities as well as the resulting friction coefficient. Both distributions are near-Gaussian, with a slight tail to the higher velocities/lower friction coefficients. The particle velocities showed a mean of 18·8 m s^{-1} and a standard deviation of 1·9 m s^{-1} and the friction coefficients showed a mean of 0·36 and a standard deviation of 0·1.

Since the velocity profile was near-Gaussian, it is not surprising that the friction coefficient profile is similar. Although this suggests that the process of particle manufacturing and acceleration in a spreader is not well controlled, it is an advantage even a necessary property. Particles with a low friction coefficient will be discharged early, at a small discharge angle with respect to the drop location. Particles with a higher friction coefficient remain longer on the disc and are discharged later at a larger discharge angle. The near-Gaussian

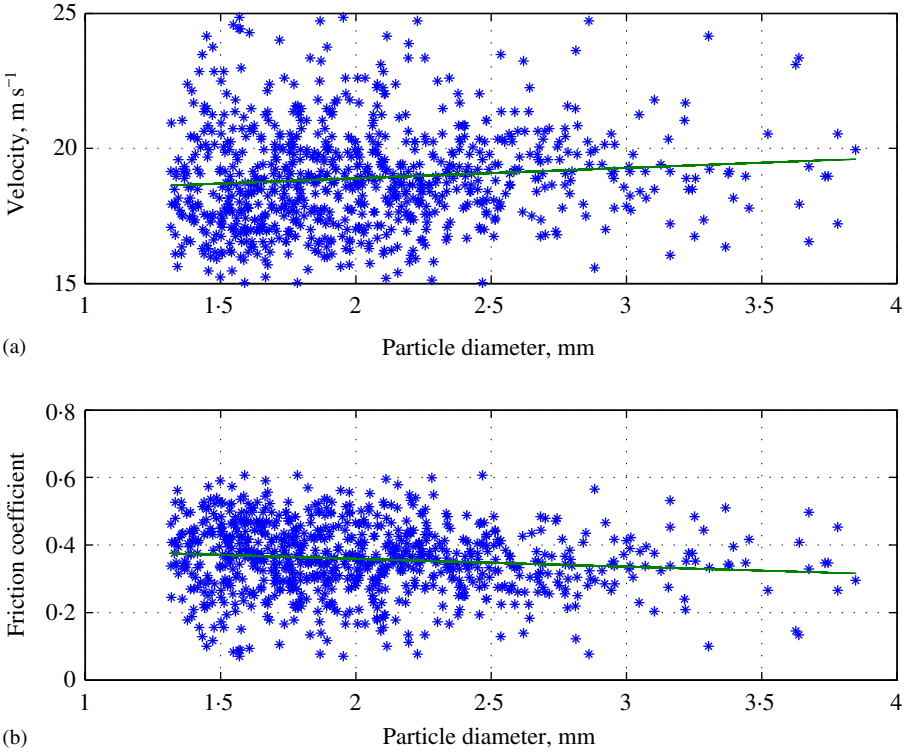

Fig. 3. (a) Measured radial velocities as a function of particle diameter with an intercept of 18·12 and slope 0·357. (b) Friction coefficients as a function of particle diameter with an intercept of 0·41 and slope −0·023. The total number of measurements was 812

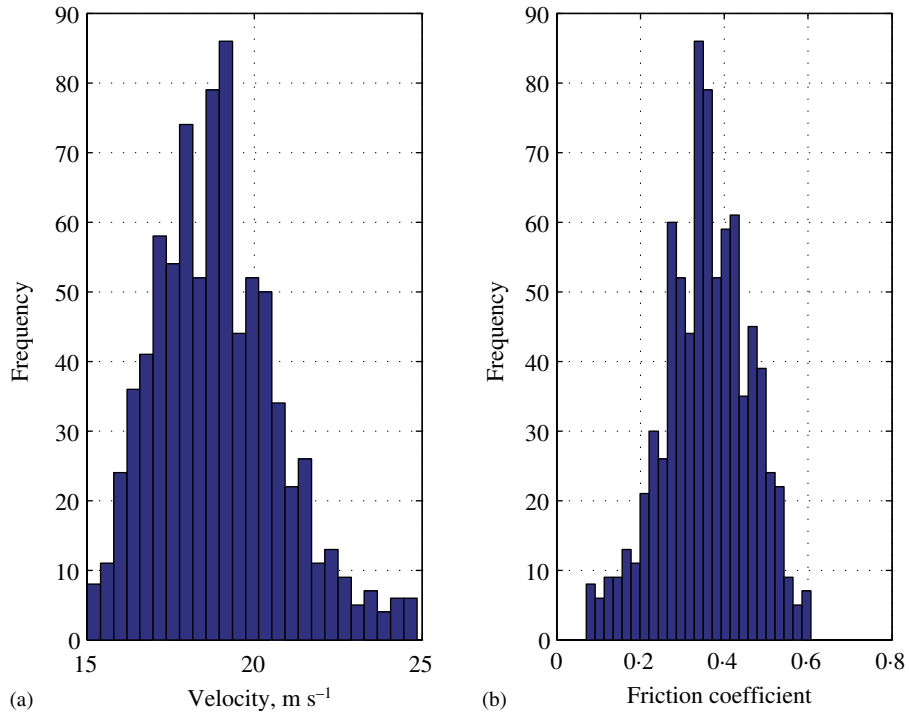

Fig. 4. (a) Histogram of measured radial velocities with a mean of 18·8 m s^{-1} and a standard deviation of 1·9 m s^{-1}; (b) histogram of friction coefficients with a mean of 0·36 and a standard deviation of 0·1

distributed friction coefficients imply near-Gaussian distributed discharge angles, which allow for producing a good pattern when properly overlapped.

4. Conclusions

To determine the dynamic mechanical (Coulomb) friction coefficient of individual urea fertiliser particles in real time, a method based on theoretical analysis was proposed. The analysis showed that the friction coefficients can be measured using a single radial velocity measurement per particle at a distance of 0·4 m from the edge of the disc.

Experiments were carried out using a modified commercial single-disc spreader. The conical disc was replaced with a flat disc with four straight radial vanes, to accommodate a simple dynamics model, which ignored aerodynamic effects on and off-disc.

The friction coefficients found for urea fertiliser showed a near-Gaussian distribution with a mean of 0·36 and a standard deviation of 0·1. The data showed that larger particles attained slightly higher velocities than smaller ones, and hence, the friction coefficients showed a moderate inverse relationship with the particle diameter.

Acknowledgements

This work was supported by a grant from the University of Illinois Research Board.

References

Aphale A; Bolander N; Park J; Shaw L; Svec J; Wassgren C (2003). Granular fertiliser particle dynamics on and off a spinner spreader. Biosystems Engineering, **85**(3), 319–329, doi:10.1016/S1537-5110(03)00062-X

ASAE Standards, ASAE (1999). S341.2. Procedure for Measuring Distribution Uniformity and Calibrating Granular Broadcast Spreaders, 46th Edn. ASAE, St. Joseph, MIC

Cunningham F M (1963). Performance characteristics of bulk spreaders for granular fertilizer. Transactions of the ASAE, **6**(2), 108–114

Dintwa E; Tijskens E; Olieslagers R; De Baerdemaeker J; Ramon H (2004b). Calibration of a spinning disc spreader simulation model for accurate site-specific fertiliser application. Biosystems Engineering, **88**(1), 49–62, doi:10.1016/j.biosystemseng.2004.01.001

Dintwa E; Van Liedekerke P; Olieslagers R; Tijskens E; Ramon H (2004a). Model for simulation of particle flow on a centrifugal fertiliser spreader. Biosystems Engineering, **87**(4), 407–415, doi:10.1016/j.biosystemseng.2003.12.009

Fulton J P; Shearer S A; Chabra G; Higgins S F (2001). Performance assessment and model development of a

variable–rate, spinner–disc fertilizer applicator. Transactions of the ASAE, **44**(5), 1071–1081

Grift T E (2000). Spread Pattern Analysis Tool (SPAT)—part 1. development and theoretical examples. Transactions of the ASAE, **43**(6), 1341–1350

Grift T E; Hofstee J W (1997). Measurement of velocity and diameter of individual fertilizer particles by an optical method. Journal of Agricultural Engineering Research, **66**(3), 235–238, doi:10.1006/jaer.1996.0128

Grift T E; Hofstee J W (2002). Testing an online spread pattern determination sensor on a broadcast fertilizer spreader. Transactions of the ASAE, **45**(3), 561–567

Grift T E; Walker J T; Gardisser D R (2000). Spread Pattern Analysis Tool (SPAT)—part 2. Examples of aircraft pattern analysis. Transactions of the ASAE, **43**(6), 1351–1363

Helms R S; Siebenmorgen T J; Norman R J (1987). The influence of uneven preflood nitrogen distribution on grain yields of rice. Arkansas Farm Research, University of Arkansas March–April

Hofstee J W (1992). Handling and spreading of fertilizers—part 2: physical properties of fertiliser, measuring methods and data. Journal of Agricultural Engineering Research, **53**(1), 141–162, doi:10.1016/0021-8634(92)80079-8

Inns F M; Reece A R (1962). The theory of the centrifugal distributor—II: motion on the disc, off-centre feed. Journal of Agricultural Engineering Research, **7**(4), 345–353

Olieslagers R; Ramon H; De Baerdemaeker J (1996). Calculation of fertilizer distribution patterns from a spinning disc spreader by means of a simulation model. Journal of Agricultural Engineering Research, **63**(2), 137–152, doi:10.1006/jaer.1996.0016

Parish RL (2002). Rate setting effects on fertilizer spreader distribution patterns. Applied Engineering in Agriculture, **18**(3), 301–304

Villette S (2005). Centrifugal fertiliser spreading: determination of the outlet velocity using motion blurred images—1st International Symposium on Centrifugal Fertiliser Spreading, 15–16 September 2005, Leuven, Belgium.

Villette S; Cointault F; Piron E; Chopinet B (2005). Centrifugal spreading: an analytical model for the motion of fertilizer particles on a spinning disc. Biosystems Engineering, **92**(2), 157–164, doi:10.1016/j.biosystemseng.2005.06.013

Appendix A: Derivation of measurement equations

The simplest model of a particle, sliding along a straight radial vane mounted on a flat spinning disc can be obtained by ignoring friction effects. This leaves only the centrifugal force acting on the particle, resulting in its acceleration as follows

$$m\ddot{x} = m\omega^2 x \tag{A1}$$

where: m is the mass of the particle in kg; x is the radial location of the particle along the vane in m; $\ddot{x}$ is the radial acceleration of the particle along the vane in $\mathrm{m\,s^{-2}}$; and ω is the rotational velocity of the disc in $\mathrm{rad\,s^{-1}}$. The solution of Eqn (A1) is

$$x(t)\big|_{\mu=0} = A\mathrm{e}^{\omega t} \tag{A2}$$

where $x(t)\big|_{\mu=0}$ is the particle location along the vane in m for a friction coefficient $\mu = 0$, t is time in s and A is an integration constant. Initially, at $t = 0$, the particle is located at R_0 in m, an arbitrary small distance from the centre of the disc. Applying the boundary condition $x(0) = R_0$ yields

$$x(t)\big|_{\mu=0} = R_0\mathrm{e}^{\omega t} \tag{A3}$$

The radial velocity of the particle $\dot{x}(t)\big|_{\mu=0}$ in $\mathrm{m\,s^{-1}}$ for a friction coefficient $\mu = 0$ as a function of time in s follows from differentiation

$$\dot{x}(t)\big|_{\mu=0} = \omega R_0\mathrm{e}^{\omega t} \tag{A4}$$

Substitution of Eqn (A3) into Eqn (A4) shows that whilst neglecting friction, the radial velocity $\dot{x}(t)\big|_{\mu=0}$ is equal to the tangential velocity $\omega x(t)\big|_{\mu=0}$ at any point along the straight radial vane

$$\dot{x}(t)\big|_{\mu=0} = \omega x(t)\big|_{\mu=0} \tag{A5}$$

For the situation with mechanical friction ($\mu > 0$), the equation of motion contains two more terms owing to friction driven by gravity (F_g) and Coriolis (F_{cor}) forces in N. The force equilibrium on the particle is now

$$m\ddot{x} = m\omega^2 x - \mu F_g - \mu F_{cor} \tag{A6}$$

The gravity and Coriolis forces in N can be written as follows

$$\begin{aligned} F_g &= mg \\ F_{cor} &= 2m\omega\dot{x} \end{aligned} \tag{A7}$$

where g is the gravitational acceleration in $\mathrm{m\,s^{-2}}$. Substitution of Eqn (A7) into Eqn (A6) leads to the equation of motion of a particle sliding along a straight radial vane as derived by Inns and Reece (1962)

$$\ddot{x} + 2\mu\omega\dot{x} - \omega^2 x = -\mu g \tag{A8}$$

The complementary function of this equation is

$$x(t) = Ae^{\omega\left(-\mu+\sqrt{\mu^2+1}\right)t} + Be^{\omega\left(-\mu-\sqrt{\mu^2+1}\right)t} \tag{A9}$$

where A and B are integrations constants. A particular solution of Eqn (A9) is $x(t) = \mu g/\omega^2$ leading to the general solution

$$x(t) = Ae^{\omega\left(-\mu+\sqrt{\mu^2+1}\right)t} + Be^{\omega\left(-\mu-\sqrt{\mu^2+1}\right)t} + \frac{\mu g}{\omega^2} \tag{A10}$$

Gravity causes a friction of the particle with the disc, but since particles move along the 'bottom' of the vane they usually do not contact the disc. This behavior is exacerbated since the gravitational force is small compared to the Coriolis force, the ratio being

$$\frac{F_g}{F_{cor}} = \frac{mg}{2m\omega\dot{x}} = \frac{g}{2\omega\dot{x}} \tag{A11}$$

Equation (A11) implies that at a rotational disc speed of $78\,\mathrm{rad\,s^{-1}}$ as used in the experiments, at a very small particle velocity of $\dot{x} = g/2\omega = 9{\cdot}81/2 \times 78 = 0{\cdot}063\,\mathrm{m\,s^{-1}}$, the gravity and Coriolis forces are equal. At the disc edge where the particles reach more than $15\,\mathrm{m\,s^{-1}}$, the Coriolis force is $2\omega\dot{x}/g = 2 \times 78 \times 15/9{\cdot}81 = 238$ times the gravity force. Hence, the gravity term was ignored which reduces the model to

$$x(t)\big|_{\mu>0} \cong Ae^{\omega\left(-\mu+\sqrt{\mu^2+1}\right)t} + Be^{\omega\left(-\mu-\sqrt{\mu^2+1}\right)t} \tag{A12}$$

The second term in Eqn (A12) contains a definite negative exponent $\left(-\mu-\sqrt{\mu^2+1}\right) < 0$, whereas the first term contains a definitive positive exponent $\left(-\mu+\sqrt{\mu^2+1}\right) > 0$. This implies that the second term vanishes quickly over time and

its effect is small at the edge of the disc and consequently at the sensor. A reasonable approximation of Eqn (A12) is now (for clarity, the equal sign ' = ' was used rather than 'equal by approximation', '≅')

$$x(t)\big|_{\mu>0} = A\mathrm{e}^{\omega\left(-\mu+\sqrt{\mu^2+1}\right)t} \tag{A13}$$

The resulting discrepancy between using the full model [Eqn (A12)] and the approximated model [Eqn (A13)] depends on the friction coefficient. If the friction coefficient is 0, the discrepancy becomes 0, since in this case the model reduces to Eqn (A3). Simulations using the full and complete model have shown that in the experimental case consisting of a flat disc with a diameter of 0·245 m, spinning at 78 rad s^{-1}, at an assumed particle friction coefficient of 0·4, the discrepancy is 0·11% at the disc edge.

For convenience, a constant κ was defined termed the exponential coefficient as follows

$$\kappa = -\mu + \sqrt{\mu^2+1} \tag{A14}$$

This definition transforms Eqn (A13) to

$$x(t)\big|_{\mu>0} = A\mathrm{e}^{\omega\kappa t} \tag{A15}$$

The radial velocity with friction $\dot{x}(t)\big|_{\mu>0}$ in m s^{-1} can be obtained from differentiation as

$$\dot{x}(t)\big|_{\mu>0} = A\omega\kappa\mathrm{e}^{\omega\kappa t} \tag{A16}$$

Substituting Eqn (A15) into Eqn (A16) yields

$$\dot{x}(t)\big|_{\mu>0} = \kappa\omega x(t)\big|_{\mu>0} \tag{A17}$$

At the edge of the disc where $x(t)\big|_{\mu>0} = R$ in m, the particle will now have a radial discharge velocity $\dot{x}(t)\big|_{\mu>0} = v_{RAD}$ in m s^{-1} as follows

$$v_{RAD} = \omega R\kappa \tag{A18}$$

The tangential velocity v_{TAN} in m s^{-1} is assumed constant and equal to the tangential velocity of the vane at the disc edge since the particle is assumed in contact with the vane until emanation

$$v_{TAN} = \omega R \tag{A19}$$

The friction angle ε in rad was defined as [Eqns (A18) and (A19)]

$$\varepsilon = \tan^{-1}\left(\frac{v_{RAD}}{v_{TAN}}\right) = \tan^{-1}(\kappa) \tag{A20}$$

To obtain the sensor angle β in rad, the sine rule was applied to the triangle with angles α,$(\pi/2+\varepsilon)$,β where α is the discharge angle in rad, yielding

$$\frac{\sin\left(\pi/2+\varepsilon\right)}{(R+D)} = \frac{\sin\beta}{R} \tag{A21}$$

where D is the radial distance in m between the sensor and the disc edge. Combining Eqns (A20) and (A21) yields

$$\beta = \sin^{-1}\left[\frac{R}{(R+D)}\sin\left(\frac{\pi}{2}+\underbrace{\tan^{-1}(\kappa)}_{\varepsilon}\right)\right] \tag{A22}$$

With $\sin\left(\pi/2+\tan^{-1}(\kappa)\right) = \cos\left(\tan^{-1}(\kappa)\right)$ Eqn (A22) reduces to

$$\beta = \sin^{-1}\left[\frac{R}{(R+D)}\cos\left(\tan^{-1}(\kappa)\right)\right] \tag{A23}$$

Considering $\cos\left(\tan^{-1}(\kappa)\right) = \frac{1}{\sqrt{1+\kappa^2}}$ Eqn (A23) reduces to

$$\beta = \sin^{-1}\left[\frac{R}{(R+D)}\frac{1}{\sqrt{1+\kappa^2}}\right] \tag{A24}$$

The total discharge velocity v_{TOT} is [*Fig. 1* and Eqns (A18) and (A19)]

$$v_{TOT} = \sqrt{v_{RAD}^2 + v_{TAN}^2} = \omega R\sqrt{1+\kappa^2} \tag{A25}$$

Since aerodynamic friction is ignored, the total measured velocity is equal to the total discharge velocity or

$$u_{TOT} = v_{TOT} \tag{A26}$$

The tangential discharge velocity at the measurement point u_{TAN} can be computed as follows

$$u_{TAN} = u_{TOT}\sin\beta \tag{A27}$$

Substitution of Eqns (A24)–(A26) into Eqn (A27) gives

$$u_{TAN} = \overbrace{\omega R\sqrt{1+\kappa^2}}^{u_{TOT}}\sin\left(\overbrace{\sin^{-1}\left[\frac{R}{(R+D)}\frac{1}{\sqrt{1+\kappa^2}}\right]}^{\beta}\right) \tag{A28}$$

Since the arcsine and sine cancel, Eqn (A28) reduces to

$$u_{TAN} = \omega R\frac{R}{R+D} = v_{TAN}\frac{R}{R+D} \tag{A29}$$

Equation (A29) shows that whilst ignoring aerodynamic friction effects, the tangential discharge velocity at the measurement location is independent of mechanical friction even though the sensor is not placed at the disc edge.

The radial particle velocity at the measurement point u_{RAD} was measured using the optical sensor. Theoretically, this velocity is equal to

$$u_{RAD} = \left[u_{TOT}^2 - u_{TAN}^2\right]^{1/2} \tag{A30}$$

Substitution of Eqns (A25), (A26), and (A29) gives

$$u_{RAD} = \left[\left(\omega R\sqrt{1+\kappa^2}\right)^2 - \left(\omega R\frac{R}{R+D}\right)^2\right]^{1/2} \tag{A31}$$

Simplification yields

$$u_{RAD} = \omega R\left[1+\kappa^2 - \left(\frac{R}{R+D}\right)^2\right]^{1/2} \tag{A32}$$

Solving Eqn (A32) for κ gives

$$\kappa = \left[\left(\frac{u_{RAD}}{\omega R}\right)^2 + \left(\frac{R}{R+D}\right)^2 - 1\right]^{1/2} \tag{A33}$$

Since the exponential coefficient κ is merely a function of the measured radial velocity u_{RAD} in m s^{-1} as well as the constants ω,R,D it can be directly computed after each measurement. The friction coefficient can be obtained by

solving Eqn (A14) for μ

$$\mu = \frac{1}{2}\left(\frac{1}{\kappa} - \kappa\right) \tag{A34}$$

The travel distance through air L_{AIR} in m can be computed as follows: since κ and consequently ε and β are known [Eqns (A33), (A20) and (A24)], the discharge angle α in rad follows from the sum of angles in a triangle

$$\alpha + \left(\frac{\pi}{2} + \varepsilon\right) + \beta = \pi \tag{A35}$$

or

$$\alpha = \frac{\pi}{2} - \beta - \varepsilon \tag{A36}$$

Applying the sine rule yields the total distance of the particle travelling through air from the discharge point to the sensor location L_{AIR}.

$$\frac{L_{AIR}}{\sin\alpha} = \frac{R}{\sin\beta} \tag{A37}$$

Since

$$\sin\alpha = \sin\left(\frac{\pi}{2} - (\beta + \varepsilon)\right) = \cos(\beta + \varepsilon) \tag{A38}$$

L_{AIR} can be written as

$$L_{AIR} = R\frac{\cos(\beta + \varepsilon)}{\sin\beta} \tag{A39}$$

Using the equality

$$\cos(\beta + \varepsilon) = \cos\beta\cos\varepsilon - \sin\beta\sin\varepsilon \tag{A40}$$

and writing all terms as a function of κ (*Fig. 1*) as follows yields

$$\sin\beta = \frac{u_{TAN}}{u_{TOT}} = \frac{R}{(R+D)}\frac{1}{\sqrt{1+\kappa^2}} \tag{A41}$$

$$\cos\beta = \frac{u_{RAD}}{u_{TOT}} = \frac{\sqrt{1+\kappa^2 - \left(\frac{R}{R+D}\right)^2}}{\sqrt{1+\kappa^2}} \tag{A42}$$

$$\cos\varepsilon = \frac{v_{TAN}}{v_{TOT}} = \frac{v_{TAN}}{u_{TOT}} = \frac{1}{\sqrt{1+\kappa^2}} \tag{A43}$$

$$\sin\varepsilon = \frac{v_{RAD}}{v_{TOT}} = \frac{v_{RAD}}{u_{TOT}} = \frac{\kappa}{\sqrt{1+\kappa^2}} \tag{A44}$$

Substitution and simplification leads to

$$L_{AIR} = \frac{1}{\sqrt{1+\kappa^2}}\left[(R+D)\sqrt{1+\kappa^2 - \left(\frac{R}{R+D}\right)^2} - \kappa R\right] \tag{A45}$$